Modulation of G-protein activation, calcium currents and opioid receptor phosphorylation by the pH-dependent agonist NFEPP

Melih Celik[1], Viola Seitz[1], Fatih Yergoz[1], Sandeep Dembla[1], Nina Blum[2], Stefan Schulz[2], and Christoph Stein[1]

[1]Charite Universitatsmedizin Berlin
[2]Universitätsklinikum Jena

July 5, 2022

Abstract

Abstract Background and Purpose NFEPP is a newly-designed pain killer selectively activating G-protein coupled mu opioid receptors in injured tissues, and therefore devoid of central side effects. However, the cellular mechanisms underlying NFEPP's antinociceptive effects were not examined in sufficient detail so far. Here we investigated the effects of NFEPP on G-protein activation, on voltage gated calcium channels and on mu opioid receptor phosphorylation. Experimental Approach HEK293 cells stably transfected with mu opioid receptors were used to study [35S]-GTPγS binding and mu opioid receptor phosphorylation. Voltage dependent calcium currents and intracellular calcium signals were examined in rat sensory neurons. All experiments were performed at acidic and physiological pH values using NFEPP compared to the conventional mu opioid receptor agonist fentanyl. To investigate the role of G protein subunits, we used pertussis toxin and gallein. Key Results At low pH, NFEPP produced more efficient G-protein activation and reduction of calcium currents in depolarized sensory neurons. The latter was mediated by G protein βγ subunits and NFEPP-mediated MOR phosphorylation was pH-dependent. Fentanyl-induced signaling was not affected by pH changes. Conclusion and Implications Our study shows that, at low pH, MOR signaling induced by NFEPP is more effective and neuronal calcium channels are directly modulated by G protein βγ subunits dissociated from G protein αi/o subunits. Apparently, the enhanced efficacy of NFEPP is dependent on extra- rather than intracellular effects on opioid receptor function.

Introduction

Opioids are the strongest painkillers to date. Clinically used opioid drugs (e.g. morphine, fentanyl) mainly target the mu opioid receptor (MOR), a G-protein coupled receptor (GPCR). The activation of MORs in the peripheral (PNS) and central nervous system (CNS) produces strong pain relief, but their activation in the CNS also results in serious side effects including addiction and respiratory depression (Imam et al., 2018). Recently, our group designed a new MOR agonist, (±)-N-(3-fluoro-1-phenethylpiperidine-4-yl)-N-phenyl propionamide (NFEPP), with a lower acid dissociation constant (pK_a) (Spahn et al., 2017; Rosas et al., 2019; Lešnik et al., 2020; Ray et al., 2020). NFEPP selectively activated peripheral MORs in inflamed tissues at low pH values (common in most painful injuries) whereas a conventional opioid (fentanyl) was equally active at both low and normal pH values (Spahn et al., 2017; Rodriguez-Gaztelumendi et al., 2018; Stein, 2018; Del Vecchio et al., 2019; Jiménez-Vargas et al., 2022). Targeting opioid receptors in the PNS at the site of injury avoids CNS side effects, while still contributing to strong analgesia, as previously demonstrated in preclinical and clinical studies: (i) locally applied opioids relieve severe clinical pain and a large proportion of the analgesic effects of systemically administered opioids is mediated by opioid receptors in the PNS (Jagla et al., 2014; Machelska and Celik, 2018; Martínez and Abalo, 2020); (ii) input from peripheral sensory neurons is essential in numerous pain syndromes (Berta et al., 2017; Sexton et al., 2018); (iii) upon injury, MOR expression is upregulated in peripheral sensory neurons and the perineurial barrier

is disrupted, eventually increasing accessibility of the drugs' target (reviewed in Machelska and Celik, 2018; Jeske, 2019).

So far, the mechanisms underlying NFEPP-induced antinociception were not examined in sufficient detail. At the level of sensory neurons, voltage dependent Ca^{2+} channels (VDCC) play a major role in the generation and inhibition of pain. These channels regulate the excitation of neurons by allowing Ca^{2+} influx into the neuron (Lu and Ikeda, 2016; Weiss and Zamponi, 2021). Following the activation of MOR and dissociation of the heterotrimeric G-protein complex, $G_{\beta\gamma}$ subunits block VDCC function, leading to decreased excitability of the sensory neuron (Proft and Weiss, 2015; Lu and Ikeda, 2016). Finally, MOR is phosphorylated and internalized (Machelska and Celik, 2018; Jeske, 2019; Mann et al., 2015).

In this study, we investigated the effects of NFEPP at acidic and physiological pH in comparison to the conventional agonist fentanyl on G-protein activation, on the activity of endogenous VDCCs and on MOR phosphorylation.

Methods

Animals

Animal experiments were approved by the State animal care committee (Landesamt für Gesundheit und Soziales, Berlin, Germany) and followed the ARRIVE guidelines (Kilkenny et al., 2010). Male Wistar rats (200-300 g; Janvier, Le Genest-Saint-Isle, France) were housed in groups of 1-2 per cage in a 12 h light/dark cycle, lined with ground corncob bedding and with free access to standard laboratory rodent chow and tap water. Room temperature was 22 ± 0.5*C and humidity was 60–65%. We investigated males only because the current evidence on gender- or sex-differences in opioid analgesia is not strong enough to warrant gender- or sex-specific therapeutic interventions (Bruehl et al., 2013; Fullerton et al., 2018).

Chemicals and Drugs

NFEPP was synthesized and provided by ASCA GmbH (Berlin, Germany) as described in (Spahn, Del Vecchio et al. 2017). Fentanyl citrate (F3886) and naloxone hydrochloride (NLX; N7758), were purchased from Sigma-Aldrich (Taufkirchen, Germany). Pertussis toxin (PTX) and gallein were purchased from Tocris (Wiesbaden-Nordenstadt, Germany). Radioactively labeled GTPγS kits were purchased from Perkin Elmer (Freiburg, Germany).

Chemicals used for membrane preparation and [^{35}S]-guanosine-5'-O-(3-thio)-triphosphate ([^{35}S]-GTPγS) binding: Trizma® Preset Crystals (Sigma-Aldrich, Taufkirchen, Germany), bovine serum albumin (BSA), dithiotreitol (DTT), GDP, [^{35}S]-GTPγS, GTPγS, optiphase HISAFE 3 (Perkin Elmer, Waltham, USA); HEM G-protein buffer: 8 mM HEPES, 8 mM EPPS, 8 mM MES, 100 mM NaCl, 0.2 mM EGTA, 5 mM $MgCl_2$; all from Sigma-Aldrich (Taufkirchen, Germany).

Chemicals used for dissociation and culture of sensory neurons: Dulbecco's Modified Eagles Medium (DMEM)/HAM's F-12 medium (Biochrom F4815, Berlin, Germany), Penicillin (10,000 U), Streptomycin (10 mg/ml), 1.25% Collagenase (Sigma-Aldrich, Taufkirchen Germany), 2.5% Trypsin (Sigma-Aldrich, Taufkirchen, Germany), acridine orange/propidium iodide (Logos, Villeneuve, France).

Chemicals used for patch clamp experiments: Extracellular buffer (ECS) (10 mM $CaCl_2 \cdot 6H_2O$, 130 mM TEA-Cl_2, 5 mM HEPES, 25 mM d-glucose; adjusted to pH 7.4 or 6.5; all from Sigma-Aldrich, Taufkirchen, Germany). Intracellular buffer (ICS) (105 mM CsCl, 2.5 mM $MgCl_2$, 40 mM HEPES, 10 mM EGTA, 2 mM Mg-ATP, 0.5 mM GTP, 5 mM d-glucose; adjusted to pH 7.4 or 6.5; all from Sigma-Aldrich, Taufkirchen, Germany).

Chemicals used for calcium imaging: Fura 2-AM (Thermo-Fisher, Hennigsdorf, Germany). Extracellular solution: 130 mM NaCl, 3 KCl mM, 2 mM $CaCl_2$, 0.6 mM $MgCl_2$, 1 mM $NaHCO_3$ 10 mM HEPES, 5 mM D-glucose (adjusted to pH 7.4 or 6.5). High K^+ solution contained: 61 NaCl mM, 75 KCl mM, 2 $CaCl_2$ mM, 0.6 $MgCl_2$ mM, 1 $NaHCO_3$ mM, 10 Hepes mM, 5 D-glucose mM (adjusted to pH 7.4 or 6.5); all from Sigma-Aldrich (Taufkirchen, Germany).

Chemicals used for MOR phosphorylation experiments: The phosphosite-specific MOR antibodies against pT370-MOR (7TM0319B), pS375-MOR (7TM0319C), pT376-MOR (7TM0319D), and pT379-MOR (7TM0319E) as well as the phosphorylation-independent antibodies against np-MOR (7TM0319N) and rabbit polyclonal anti-HA antibodies (7TM000HA) were provided by 7TM Antibodies (Jena, Germany). [D-Ala2, N-MePhe4, Gly-ol]-enkephalin (DAMGO) acetate salt and dimethyl sulfoxide (DMSO) were purchased from Sigma-Aldrich (Darmstadt, Germany). Fentanyl citrate was obtained from Rotexmedica (Trittau, Germany).

Culture and Transfection of Human embryonic kidney (HEK) cells

Human embryonic kidney (HEK293) cells (German Collection of microorganisms and Cell Cultures, Braunschweig, Germany; RRID:CVCL_0045) were maintained in full medium containing DMEM media supplemented with fetal bovine serum (Biochrom, Berlin, Germany), penicillin (100 U/ml, Biochrom) and streptomycin (100 µg/ml, Biochrom) with or without geneticin (G418, 100 µg/ml, Biochrom), in 5% CO2 at 37 °C as described before{Spahn, 2017, nontoxic}. Cells were passaged 1:3 - 1:20 every second to third day from p8 and p28 depending on confluence.

For MOR transfection, wild-type HEK293 cells were plated on 30 mm diameter plastic culture dishes coated with poly-L-lysine 24 h before transfection. Confluent HEK293 cells (70–90%) were transfected with 1 µg per 200 µl transfection mix of each plasmid containing the different cDNAs using "X-tremeGENE HP DNA Transfection Reagent" (Roche; Mannheim, Germany) following the supplier's recommendations. The plasmid containing the cDNA encoding the FLAG-epitope-tagged rat MOR (oprm1, NM 013071.2) in pcDNA3.1 vector with geneticin resistance gene was provided by Prof. Christian Zöllner (University Hamburg, Germany). The cells were later grown in T175 flasks to have enough membranes for further experiment.

Membrane Preparation

Membrane fractions were prepared from transfected HEK293 cells as described previously (Zöllner, 2003). The cells were grown in 175 cm2 tissue culture flasks to approximately 90 % confluence. Cells were then washed with Tris buffer (50 mM, Trizma preset crystals, pH 7.4; Sigma Aldrich, Darmstadt, Germany), harvested with a scraper, homogenized using a mechanical disperser (Dispergierstation T8.10, IKA-Werke, Staufen, Germany) at maximum speed for 10 s and centrifuged at 42K x g for 20 min at 4oC (Avanti JXN-26 ultracentrifuge, Beckmann Coulter, Krefeld, Germany). Cellular pellets including membranes with embedded and anchored proteins were then resuspendend in Tris buffer for washing to separate them from cytosolic components by homogenization and centrifugation at the same settings. Supernatants were discarded and the pellets were stored at -80 oC. On the day of usage, the pellets were thawed on ice in Tris buffer and homogenized. Total protein concentrations were determined according to the Bradford method (Bio-Rad Laboratories GmbH, München, Germany). (Bradford, 1976) and homogenates were split according to the number of conditions tested in respective assay buffers.

Isolation and culture of sensory neurons

Dorsal root ganglia (DRGs) were harvested from naïve male Wistar rats following their sacrifice by an overdose of isoflurane (5%) (AbbVie, Wiesbaden, Germany). Immediately thereafter, the thoracic and lumbar spinal regions were exposed and all DRGs were collected in a working medium (DMEM/HAM's F-12 without penicillin/streptomycin). 1.25% collagenase was added just before incubation. Following their incubation at 37°C for 60 min, DRGs were washed three times with PBS and incubated in the working medium digestive solution with trypsin for 10 min at 37°C. Thereafter, the tissue was further triturated using plastic pipette tips and filtered through a 40 µl filter. The filtrate was centrifuged and the pellet was resuspended in 1 ml culture medium (DMEM/HAM's F12 supplemented with 1% penicillin/streptomycin and 10% horse serum). Neurons were then seeded onto poly-L-lysine coated plastic culture dishes (35 mm) and placed in an incubator (5% CO_2 at 37°C). One hour later, 2 ml of culture medium were added to the cell culture and neurons were incubated for 24–48 h until patch clamp recordings or calcium imaging, as previously described (Nockemann et al., 2013; Dembla et al., 2017).

[35Σ]-ΓΤΠγΣ βινδινγ εξπεριμεντς

[35S]-GTPγS experiments were performed on crude membrane fractions of MOR-expressing HEK293 cells to determine mu-agonist-induced G-protein activation (as reflected by the exchange rate of GDP for GTP) at different pH values (6.5-7.4). GTP was replaced by a high concentration of [35S]-GTPγS in the assay solvent, and the accumulation of [35S]-GTPγS-bound G proteins in the membrane was measured. To this end, membranes were homogenized and dissolved in HEM G-protein buffer at pH 7.4 or 6.5, including freshly added 0.1 % (w/v) BSA and 1 mM dithiotreitol (DTT). In analogy to (Ludwig et al., 2003), 50 µg of membrane fractions in duplicates were incubated with GDP (30 µM) and [35S]-GTPγS (0.05 nM) for 90 min at 30°C to determine dose-response curves and EC_{50} values. Unspecific [35S]-GTPγS binding in the presence of non-radioactive GTPγS (10 µM) was subtracted to yield specific binding. Bound and free ligands were separated by rapid filtration under vacuum through Whatman GF/B glass fibre filters soaked in water followed by 6 washes with Tris Buffer. Bound radioactivity was determined by liquid scintillation spectrophotometry for 35S after overnight extraction of the filters in scintillation fluid *optiphase HISAFE3* . Concentrations of radioactive compound were calculated based on the half-life of 35S (87.4 days). Experiments were randomized to compensate for position effects in the filter apparatus or unequal sample processing times. Data processing and analysis were blinded for pH values (6.5 or 7.4) with the help of a colleague.

Patch clamp experiments

Patch clamp experiments were performed on rat sensory neurons (DRGs) 24–48 h after their dissection, following a modified protocol from (Walwyn et al., 2007). First, cell viability was evaluated by an automated cell counter (Luna, Villeneuve, France) using acridine orange/propidium iodide dyes. During patch clamp recordings, cells were superfused with ECS buffer and visualized using a Zeiss Axiovert 200 inverse microscope (Zeiss, Jena, Germany). Patch clamp pipettes (resistance 3.5–8 MΩ) were produced using the Sutter P-97 puller (Sutter Instruments, Novato, CA, USA) from Borosilicate glass capillaries (Harvard Bioscience, MA, USA). Before the experiment, the glass pipettes were filled with an ICS buffer. Currents were amplified by an EPC-10 patch amplifier and recorded using Pulse software (HEKA, Lambrecht, Germany). Using a pressurized application system (Perfusion Pressure Kit VPP-6; Warner Instruments, Hamden, CT, USA), ECS buffer was added in a steady flow of 800–1,000 µl/min. After reaching the "giga-seal" at -60 mV, the membrane patch was breached to achieve the whole-cell configuration. The currents were initially recorded at a holding potential of -80 mV in ECS buffer in the absence of test compounds. Subsequently, the cells were depolarized to +10 mV (for 100 ms) for eight times following 20 s intervals. During the first five cycles, only ECS buffer continued to flow. On the sixth cycle, an opioid agonist (fentanyl, NFEPP) was added to the solution. During the last two cycles, the opioid antagonist naloxone was used to block/confirm opioid receptor-mediated effects. Neurons were selected for analysis after the 8^{th} cycle. For experiments using PTX or gallein, the blockers were added to culture media overnight before the day of the experiment (Lu and Ikeda 2016). Opioid ligands were administered via a perfusion valve system (VC-6; Warner Instruments). All recordings were performed at room temperature.

Calcium Imaging

Intracellular calcium imaging experiments were performed as previously described (Dembla, Behrendt et al. 2017). Briefly, cultured rat sensory neurons (DRGs) were incubated at room temperature with 5 µM Fura 2-AM (1 mM stock in DMSO + 0.02% pluronic F-127) for 30 min in growth medium. Following the application of Fura 2-AM, cover-slips were transferred to a closed recording chamber (Warner Instruments) and continuously perfused with the extracellular solution for 5 min. Fluorescence was monitored every 2 seconds and images were taken with the DS-Qi1 (Nikon, Japan) at 510 nm wavelength. Alternate excitation at 340 and 380 nm wavelengths were filmed using a Polychrome V monochromator, mounted on a Nikon TE2000 inverted microscope (with 20x Sfluor objective; N.A. 0.5). After a baseline period of ca. 2 minutes, ligands (as shown in figures) were superfused onto the cells, using a gravity-driven perfusion system, which was controlled by ALA VC3-8 valve control system. Fluorescence intensities of ratio images (340/380 nm) on regions of interest (ROI) (including the whole cell) were quantified by NIKON NIS-Elements software

after subtraction of background. To distinguish between neuronal and non-neuronal cells, a high potassium (high K^+) solution was used to depolarize the cells at the end of the superfusion protocol.

MOR phosphorylation experiments:

HEK293 cells stably expressing MOR were cultivated at 37°C, 5% CO_2 in Dulbecco's Modified Eagle's Medium (DMEM), supplemented with 10% (v/v) fetal bovine serum (FBS), 1% (v/v) penicillin/streptomycin and 1% (v/v) glutamine (Capricorn Scientific, Ebsdorfergrund, Germany). Cells were seeded into poly-L-lysine-coated 60 mm culture dishes and grown until a confluency of 95% was reached. MOR agonists were diluted in PBS buffer of different pH values ranging from 6.0 to 8.0 and were carefully added onto the cell layer for 10 min at room temperature. After the agonist solution was removed, cells were washed with Dulbecco's PBS, with Ca^{2+} and Mg^{2+} (Capricorn Scientific, Ebsdorfergrund, Germany) and lysed with a detergent buffer (150 mM NaCl; 50 mM Tris-HCl, pH 7.4; 5 mM EDTA; 1% Igepal CA-360; 0.5% deoxycholic acid; and 0.1% SDS) containing phosphatase and protease inhibitors (PhosSTOP and cOmplete mini tablets; Roche, Mannheim, Germany). Cell lysates were then centrifuged at 21,000 x g and 4°C for 30 min to obtain the supernatant which was mixed with HA epitope tag antibody agarose conjugates (Thermo Fisher Scientific, Waltham, USA). This mixture was incubated for 2 h at 4°C. After washing the agarose beads with detergent buffer for three times, SDS sample buffer (100 mM DTT, 62.5 mM Tris-HCl, 20% glycerol, 2% SDS, and 0.005% bromophenol blue) was added and incubated at 43°C for 25 min to release the precipitated receptor from the conjugates.

For electrophoresis, the supernatant was loaded onto an 8% polyacrylamide gel. Subsequently, the proteins were transferred to a PVDF membrane using a semi-dry blotting system (Trans-Blot® Turbo Transfer System, Bio-Rad Laboratories GmbH, Feldkirchen, Germany). Unspecific binding sites were blocked by incubating the membranes in 5% BSA/TBS-T buffer solution for 2 h at room temperature, before the primary antibody diluted in 5% BSA/TBS-T was added overnight at 4°C. On the next day, the membrane was washed three times with TBS-T and incubated with the secondary antibody diluted in 5% BSA/TBS-T for 2 h at room temperature. After washing the membrane for another three times, it was placed into SuperSignal West Dura Extended Duration Substrate (Thermo Fisher Scientific, Waltham, USA) to induce a chemiluminescent reaction. The signals were detected using Fusion Fx7 (Peqlab, Erlangen, Germany). In order to reprobe the membrane, bound antibodies were removed by Tris (2-carboxyethyl) phosphin containing stripping buffer.

Western Blot signals were quantified using the software ImageJ. The intensity of each band was calculated by subtracting the background signal from the mean intensity of the selected band area. To determine the magnitude of protein phosphorylation, the ratio of the signal of the phosphorylated protein to the one exhibited by the loading control (total protein concentration) was calculated.

Data analysis and statistics

Sample sizes were calculated using the G*Power 3.1.2 program with $\alpha < 0.05$ and a power of 80% based on a defined effect size derived from pilot experiments. Experiments were randomized to compensate for the position effects on plates or filter apparatus and unequal sample processing time. All experiments were performed by an investigator blinded to the sample assignments. The codes were broken after the completion of the experiments. Statistical analyses were performed using GraphPad Prism software (version 5 and 9 for Windows; GraphPad Software Inc., San Diego, USA). Grubbs' test was performed to identify potential outliers. No samples were excluded from the analysis. All data were assessed for normal distribution and equal variances by D'Agostino and Pearson or Kolmogorov–Smirnov tests. Analysis of concentration-response relationships was performed with simple linear regression using Prism 9 (where y = [^{35}S]-GTPγS bound and x = [NFEPP] or [fentanyl]). Ca^{2+}imaging time series of single cells were extracted from stacks of ratio images as averages over the entire cell area in excel-sheets, which were then plotted as time vs. ratio 340/380 graphs using Prism 5. For quantitative analyses, the first 10 data points (corresponding to the first 20 s of the experiment) were averaged to form the baseline which was then subtracted from all high potassium (high K^+) responding cells to obtain Δ ratio 340/380 values. During each recording, we typically were able

to record at least from 10 cells, meaning that each trace in Ca^{2+} imaging recordings represents the mean of more than 20 cells. The precise number of cells is stated in the figures or in the figure legends. Data are represented as means ± standard error of the mean (SEM). Detailed statistical analyses are presented in figure legends.

Results

Both NFEPP and fentanyl produced dose-dependent increases in [^{35}S]-GTPγS binding (Figure 1). The maximum effects of NFEPP were significantly higher and the EC_{50}values were significantly lower at pH 6.5 when compared to the physiological pH 7.4 (see Table 1; *P < 0.05; pH 6.5 versus pH 7.4; t test, N=6 and 7 membranes). In contrast, fentanyl showed similar potencies (EC_{50}) and similar maximum effects at both pH values (Figure 1, Table 1).

Table 1. EC_{50} values in [^{35}S]-GTPγS binding experiments

	NFEPP	NFEPP	Fentanyl	Fentanyl
pH	6.5	7.4	6.5	7.4
EC_{50} (mean)	1,340e-007*	7,943e-007	2,905e-008	4,709e-008
standard error	3,594e-008	2,644e-007	4,103e-009	1,081e-008

In the patch clamp experiments, the DRG cells initially rested in the whole-cell voltage clamp mode at a constant -80 mV holding potential. When depolarized to +10 mV (100 ms), VDCCs opened to allow Ca^{2+} ions to flow into the cell inducing an inward current. NFEPP treatment dose-dependently decreased VDCC currents at both pH values (6.5 and 7.4) but to different degrees. At pH 6.5, the most effective NFEPP dose (100 μM) attenuated Ca^{2+}currents by 41.8 %. This effect was significantly stronger than the effect of NFEPP at pH 7.4 (28.8%) (Figure 2a). In contrast to NFEPP, the dose-response curves upon fentanyl treatment were not different and the most effective fentanyl dose (100 μM) attenuated +10 mV-induced Ca^{2+} currents to the same degree (˜39%) at both pH 7.4 and pH 6.5 (Figure 2b). These findings show that NFEPP is more effective at low pH, whereas the conventional opioid agonist fentanyl is equally effective at both acidic and physiological pH values. Naloxone dose-dependently recovered the +10 mV-induced VDCC currents during NFEPP treatment. The effects of NFEPP were completely reversed by the highest naloxone dose (100 μM) at both pH values (Figure 3a). This dose of naloxone also abolished fentanyl effects at both pH values (Figure 3b).

To investigate the role of G-protein subunits in detail, we initially used PTX which prevents the replacement of GDP by GTP at the $G_{\alpha\imath}$ subunits and precludes subsequent $G_{\alpha\beta\gamma}$ dissociation (Lu and Ikeda, 2016). PTX blocked NFEPP's effect in a dose-dependent manner (Figure 4a), fully reversing the +10 mV-induced VDCC currents at the highest PTX dose (100 ng/ml). The effect of fentanyl was also blocked in a dose-dependent manner after PTX incubation (Figure 4b). Because PTX does not allow to distinguish between the involvement of G_{α} versus $G_{\beta\gamma}$subunits (Lu and Ikeda, 2016), we sought to selectively block $G_{\beta\gamma}$ subunits by gallein (Lu and Ikeda, 2016). Gallein dose-dependently decreased NFEPP-induced effects and fully recovered +10 mV-induced Ca^{2+} currents at the highest dose at both pH values (Figure 5a). Fentanyl's effects were also decreased and fully blocked by the most effective dose of gallein at both pH values (Figure 5b). Together, these results indicate that the effects of both opioid agonists on VDCCs are mediated via activation and subsequent dissociation of heterotrimeric G-protein complexes at both pH values.

We then performed Ca^{2+} imaging experiments to corroborate our electrophysiological results. Under our recording conditions, both NFEPP and fentanyl decreased the Fura [?] ratio 340/380, i.e. the Ca^{2+} signals were reduced. Naloxone (100 μM) completely reversed the effect of fentanyl (Figure 6b, c). However, in NFEPP-treated neurons, the Ca^{2+} signal was significantly lower at pH 6.5 when compared to pH 7.4 (Figure 6a, c). We also examined whether the extracellular pH by itself had a role in the decrease of Ca^{2+} signals. During short (60 s) (Figure 7a) or long (20 min) (Figure 7b) term pH changes, there was no difference in the Fura [?] ratio 340/380 at either pH 6, 6.5, 7 or 7.4. This indicates that the pH difference by itself does not

influence Ca^{2+} signals in the cells and that NFEPP and fentanyl were solely responsible for the decrease. The control experiments using high potassium indicated that the signals indeed derived from the influx of extracellular Ca^{2+} into neurons (Figure 7).

Finally, we examined the effects of NFEPP on MOR phosphorylation. MOR expressing HEK293 cells were treated with either NFEPP or fentanyl at pH 6.0 - 8 (Figure 8a). The strongest NFEPP-mediated phosphorylation signal was detected at pH 6.0. This signal diminished with increasing pH values (Figure 8b). In contrast, fentanyl-induced phosphorylation was similar at all pH values (Figure 8c).

Discussion

Developing new analgesics with less adverse effects is challenging (reviewed in Yekkirala et al., 2017; Machelska and Celik, 2018). Activation of peripheral opioid receptors by site-restricted opioid administration was shown to produce strong analgesia in both acute and chronic pain models as well as in patients with arthritis and postoperative pain (reviewed in Machelska and Celik, 2018; Martínez and Abalo, 2020). Additionally, animal studies using conditional opioid receptor knockout in primary afferent Nav1.8 nociceptors clearly demonstrated the essential role of peripheral opioid receptors (Gaveriaux-Ruff et al., 2011; Weibel et al., 2013). Accordingly, the selective activation of peripheral MOR on DRG neurons innervating injured (inflamed) tissues appears to be a promising strategy to inhibit pain while avoiding central side effects. NFEPP is an opioid with a lower dissociation constant (pK_a) that was shown to bind and activate MORs more effectively at low pH values. Therefore, even though NFEPP is presumably distributed throughout the body (including the CNS) after systemic (intravenous) application, it only activates MORs in peripheral inflamed tissues where the pH is more acidic (reviewed in Stein, 2018).

In this study, we expanded our understanding of NFEPP's antinociceptive effects by investigating MOR signaling in transfected HEK cells and sensory neurons. Opioid receptors exert their intracellular actions through G-proteins, which interact with various cellular effector systems. First, we found that NFEPP produced more efficient G-protein activation at low pH, while fentanyl induced comparable G-protein activation at both physiological and low pH values, as shown by the [^{35}S]-GTPγS binding experiments. Opioid receptor activation can result in blockade of membrane VDCCs, which are essential for the excitation of sensory neurons (reviewed in Machelska and Celik, 2018; Weiss and Zamponi, 2021). To verify that NFEPP acts through the same mechanisms, we examined NFEPP-induced inhibition of inward calcium currents at both physiological (7.4) and acidic (6.5) pH values. Our experiments revealed that the electrical excitation of depolarized sensory neurons was more efficiently reduced following NFEPP treatment at acidic pH (in contrast to pH 7.4). However, fentanyl, a conventional opioid, attenuated Ca^{2+} currents to similar degrees at both pH values. By using naloxone, we confirmed that the effects of NFEPP and fentanyl were mediated by opioid receptors. Together, these findings support our previous studies where fentanyl, possibly due to its higher pK_a value (8.44) and comparable protonation, was equally effective at both pH values (Spahn et al., 2017, 2018). In contrast, NFEPP (pK_a = 6.82) showed increased G-protein activation and VDCC inhibition at acidic conditions, where an increase in protonation due to lower pH improves NFEPP-MOR interaction (Spahn et al. 2017). To examine whether the dissociation of G-protein subunits differs between pH values following NFEPP or fentanyl treatment, we blocked the GDP-GTP exchange at $G_{\alpha i/o}$ subunits using PTX, and we inhibited $G_{\beta\gamma}$ subunits using gallein in our patch clamp analysis. $G_{\beta\gamma}$ subunits were previously shown to directly deactivate VDCCs following MOR activation (reviewed in Proft and Weiss, 2015). Here, we have shown that NFEPP-induced inhibition of inward calcium currents were dependent on $G_{\beta\gamma}$ subunits. Consistent with its indistinguishable effect on G_{α}versus $G_{\beta\gamma}$ subunits (Lu and Ikeda, 2016), PTX also blocked Ca^{2+} currents, indicating that, by blocking GDP-GTP exchange, consequent $G_{\alpha\beta\gamma}$ dissociation is also impaired. Apparently, the extracellular pH changes did not significantly affect intracellular activation of G-proteins since the dose ranges of inhibitors (PTX, gallein) were similar for both opioid agonists and both pH values.

Further validation of our electrophysiological data was performed using Ca^{2+} imaging experiments. Ca^{2+}signals were only reduced in NFEPP-treated DRG neurons at pH 6.5. Fentanyl, however, significantly reduced Ca^{2+} signals at both pH values, indicating no difference of its efficacy between inflamed

and non-inflamed environments. Control experiments using naloxone and high potassium confirmed that the signals were modulated by opioid receptors and derived from influx of Ca^{2+} into neurons, similar to previous studies (Hochstrate et al., 1995). To examine direct effects of low pH (without drug treatment), we investigated VDCC activity at pH 6.5. Both calcium imaging and patch clamp experiments (data not shown) demonstrated that pH alone did not affect Ca^{2+} signals/ currents at low pH values.

Additionally, the ability of NFEPP to phosphorylate MOR under different pH conditions was examined. Our western blot analysis showed that NFEPP induced the strongest MOR phosphorylation at pH 6.0. The signal was most pronounced at MOR residues T370 and S375 and decreased with increasing pH levels. In comparison, fentanyl caused similar phosphorylation signals of MOR regardless of increasing pH values. Notably, the antibodies used in our experiments only detect intracellular phosphorylation sites at the C-terminal of MOR (Mann et al., 2015). Assuming that nonspecific pH effects would produce similar phosphorylation signals for all pH values and both agonists, our findings strongly suggest that the pH-dependent signals produced by NFEPP were due to extracellular pH changes. Importantly, fentanyl apparently stimulates MOR independently from extracellular pH, while NFEPP activates MOR preferentially at low pH values.

In summary, our results show that during both NFEPP and fentanyl treatment, VDCCs are directly modulated by $G_{\beta\gamma}$ subunits dissociated from $G_{\alpha/o}$. However, MOR signaling induced by NFEPP is more effective at low pH. Given the known decrease of extracellular pH in injured tissues (Stein, 2018) and the co-expression of MOR and VDCC in sensory neurons (Proft and Weiss, 2015), our study uncovers the neural mechanisms underlying the antinociceptive effects of NFEPP in injured tissues, and strongly suggests that the enhanced efficacy of NFEPP in acidic milieu is dependent on extra- rather than intracellular effects on MOR function.

References

Berta, T., Qadri, Y., Tan, P.-H., and Ji, R.-R. (2017). Targeting dorsal root ganglia and primary sensory neurons for the treatment of chronic pain. Expert Opin Ther Targets *21* : 695–703.

Bradford, M.M. (1976). A rapid and sensitive method for the quantitation of microgram quantities of protein utilizing the principle of protein-dye binding. Anal Biochem *72* : 248–254.

Bruehl, S., Apkarian, A.V., Ballantyne, J.C., Berger, A., Borsook, D., Chen, W.G., et al. (2013). Personalized medicine and opioid analgesic prescribing for chronic pain: opportunities and challenges. J Pain *14* : 103–113.

Busch-Dienstfertig, M., Roth, C.A., and Stein, C. (2013). Functional characteristics of the naked mole rat μ-opioid receptor. PLoS One *8* : e79121.

Del Vecchio, G., Labuz, D., Temp, J., Seitz, V., Kloner, M., Negrete, R., et al. (2019). pKa of opioid ligands as a discriminating factor for side effects. Sci Rep *9* : 19344.

Dembla, S., Behrendt, M., Mohr, F., Goecke, C., Sondermann, J., Schneider, F.M., et al. (2017). Anti-nociceptive action of peripheral mu-opioid receptors by G-beta-gamma protein-mediated inhibition of TRPM3 channels. Elife *6* : e26280.

Fullerton, E.F., Doyle, H.H., and Murphy, A.Z. (2018). Impact of sex on pain and opioid analgesia: a review. Curr Opin Behav Sci *23* : 183–190.

Gaveriaux-Ruff, C., Nozaki, C., Nadal, X., Hever, X.C., Weibel, R., Matifas, A., et al. (2011). Genetic ablation of delta opioid receptors in nociceptive sensory neurons increases chronic pain and abolishes opioid analgesia. Pain *152* : 1238–1248.

González-Rodríguez, S., Quadir, M.A., Gupta, S., Walker, K.A., Zhang, X., Spahn, V., et al. (2017). Polyglycerol-opioid conjugate produces analgesia devoid of side effects. ELife *6* : e27081.

Hochstrate, P., Piel, C., and Schlue, W.-R. (1995). Effect of extracellular K+ on the intracellular free Ca2+ concentration in leech glial cells and Retzius neurones. Brain Research *696* : 231–241.

Imam, M.Z., Kuo, A., Ghassabian, S., and Smith, M.T. (2018). Progress in understanding mechanisms of opioid-induced gastrointestinal adverse effects and respiratory depression. Neuropharmacology *131* : 238–255.

Jagla, C., Martus, P., and Stein, C. (2014). Peripheral opioid receptor blockade increases postoperative morphine demands–a randomized, double-blind, placebo-controlled trial. Pain *155* : 2056–2062.

Jeske, N.A. (2019). Dynamic Opioid Receptor Regulation in the Periphery. Mol Pharmacol *95* : 463–467.

Jiménez-Vargas, N.N., Yu, Y., Jensen, D.D., Bok, D.D., Wisdom, M., Latorre, R., et al. (2022). Agonist that activates the μ-opioid receptor in acidified microenvironments inhibits colitis pain without side effects. Gut *71* :695–704.

Kilkenny, C., Browne, W.J., Cuthill, I.C., Emerson, M., and Altman, D.G. (2010). Improving Bioscience Research Reporting: The ARRIVE Guidelines for Reporting Animal Research. PLOS Biology *8* : e1000412.

Lešnik, S., Hodošček, M., Bren, U., Stein, C., and Bondar, A.-N. (2020). Potential Energy Function for Fentanyl-Based Opioid Pain Killers. J. Chem. Inf. Model. *60* : 3566–3576.

Lu, V.B., and Ikeda, S.R. (2016). Strategies for Investigating G-Protein Modulation of Voltage-Gated Ca2+ Channels. Cold Spring Harb. Protoc.*5* : 426-434.

Ludwig, M.-G., Vanek, M., Guerini, D., Gasser, J.A., Jones, C.E., Junker, U., et al. (2003). Proton-sensing G-protein-coupled receptors. Nature *425* : 93–98.

Machelska, H., and Celik, M.Ö. (2018). Advances in Achieving Opioid Analgesia Without Side Effects. Front Pharmacol *9* :1388

Mann, A., Illing, S., Miess, E., and Schulz, S. (2015) Different mechanisms of homologous and heterologous μ-opioid receptor phosphorylation. Br J Pharmacol *172* : 311-316.

Martínez, V., and Abalo, R. (2020). Peripherally acting opioid analgesics and peripherally-induced analgesia. Behav Pharmacol*31* : 136–158.

Nockemann, D., Rouault, M., Labuz, D., Hublitz, P., McKnelly, K., Reis, F.C., et al. (2013). The K(+) channel GIRK2 is both necessary and sufficient for peripheral opioid-mediated analgesia. EMBO Mol Med*5* : 1263–1277.

Proft, J., and Weiss, N. (2015). G protein regulation of neuronal calcium channels: back to the future. Mol Pharmacol *87* : 890–906.

Ray, S., Sunkara, V., Schütte, C., and Weber, M. (2020). How to calculate pH-dependent binding rates for receptor–ligand systems based on thermodynamic simulations with different binding motifs. Molecular Simulation *46* : 1443–1452.

Rodriguez-Gaztelumendi, A., Spahn, V., Labuz, D., Machelska, H., and Stein, C. (2018). Analgesic effects of a novel pH-dependent μ-opioid receptor agonist in models of neuropathic and abdominal pain. Pain*159* : 2277–2284.

Rosas, R., Huang, X.-P., Roth, B.L., and Dockendorff, C. (2019). β-Fluorofentanyls Are pH-Sensitive Mu Opioid Receptor Agonists. ACS Med Chem Lett *10* : 1353–1356.

Sexton, J.E., Cox, J.J., Zhao, J., and Wood, J.N. (2018). The Genetics of Pain: Implications for Therapeutics. Annu Rev Pharmacol Toxicol*58* : 123–142.

Spahn, V., Del Vecchio, G., Labuz, D., Rodriguez-Gaztelumendi, A., Massaly, N., Temp, J., et al. (2017). A nontoxic pain killer designed by modeling of pathological receptor conformations. Science *355* : 966–969.

Spahn, V., Del Vecchio, G., Rodriguez-Gaztelumendi, A., Temp, J., Labuz, D., Kloner, M., et al. (2018). Opioid receptor signaling, analgesic and side effects induced by a computationally designed pH-dependent agonist. Sci Rep *8* : 8965.

Stein, C. (2018). New concepts in opioid analgesia. Expert Opin Investig Drugs *27* : 765–775.

Walwyn, W., Evans, C.J., and Hales, T.G. (2007). β-Arrestin2 and c-Src Regulate the Constitutive Activity and Recycling of μ Opioid Receptors in Dorsal Root Ganglion Neurons. J. Neurosci. *27* : 5092–5104.

Weibel, R., Reiss, D., Karchewski, L., Gardon, O., Matifas, A., Filliol, D., et al. (2013). Mu Opioid Receptors on Primary Afferent Nav1.8 Neurons Contribute to Opiate-Induced Analgesia: Insight from Conditional Knockout Mice. PLoS ONE *8* : e74706.

Weiss, N., and Zamponi, G.W. (2021). Opioid Receptor Regulation of Neuronal Voltage-Gated Calcium Channels. Cell Mol Neurobiol *41* : 839–847.

Yekkirala, A.S., Roberson, D.P., Bean, B.P., and Woolf, C.J. (2017). Breaking barriers to novel analgesic drug development. Nat Rev Drug Discov *16* : 545–564.

Zollner, C., Shaqura, M.A., Bopaiah, C.P., Mousa, S., Stein, C., Schafer, M. (2003). Painful inflammation-induced increase in mu-opioid receptor binding and G-protein coupling in primary afferent neurons. *Mol Pharmacol* 64(2):202-10.

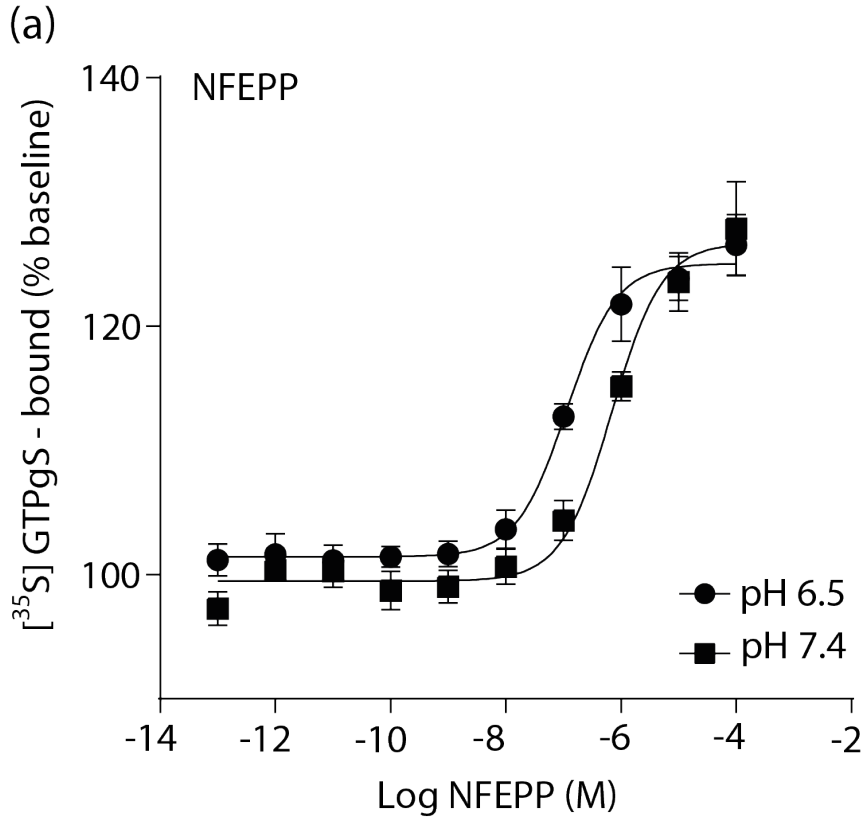

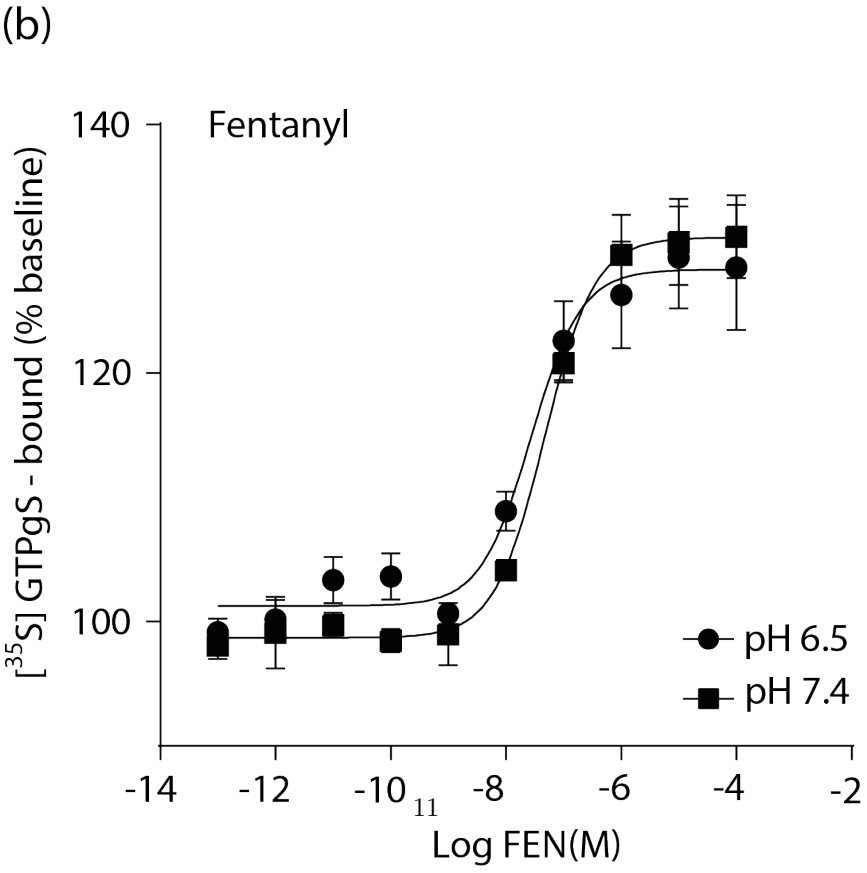

Figure 1

Dose-dependent [^{35}S]-GTPγS binding induced by NFEPP (a) and fentanyl (b) at pH 6.5 and 7.4. [^{35}S]-GTPγS binding is expressed as percent increase in [^{35}S]-GTPγS binding relative to binding in unstimulated samples (n=6 membrane preparations). Data points represent means ± standard error of the mean (SEM) of specific [^{35}S]-GTPγS binding in % of baseline. $P < 0.05$ for Log EC_{50} of NFEPP at pH 6.5 vs 7.4, 2-tailed t test.

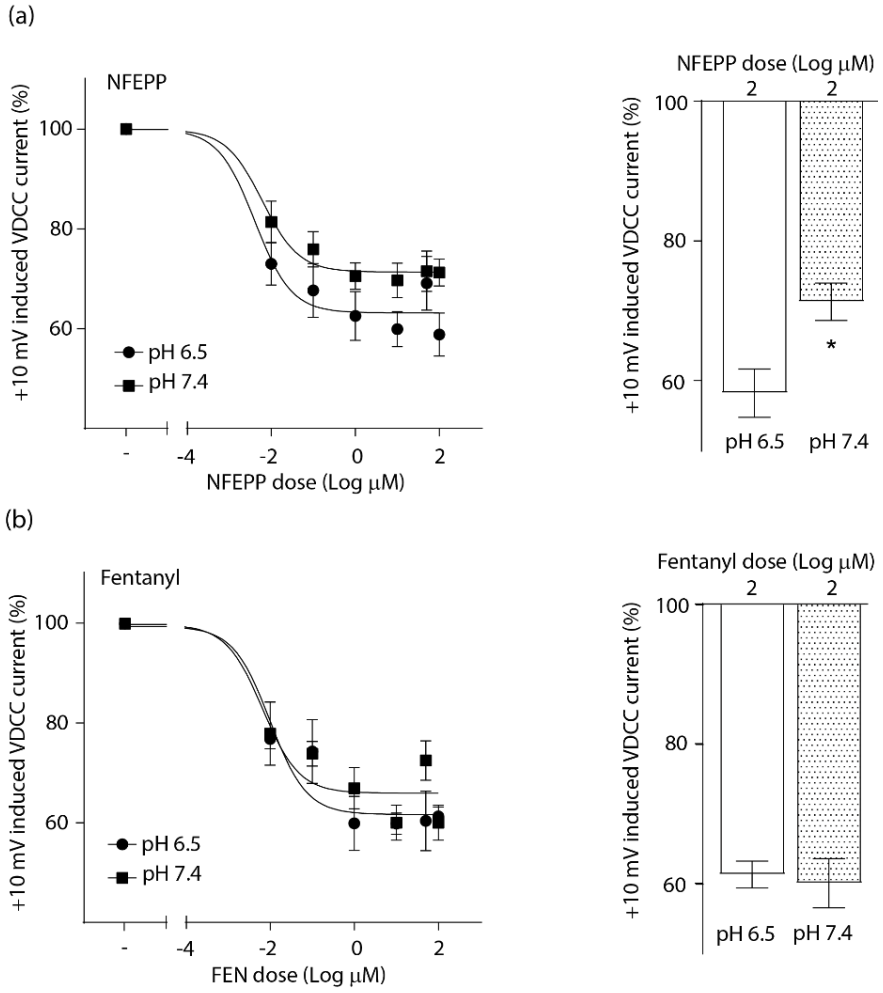

Figure 2

Dose-dependent inhibition of +10mV-induced calcium currents in isolated rat sensory neurons (DRG cells) by NFEPP (a) or fentanyl (b) at pH 6.5 and pH 7.4 measured by patch clamp (N=14-22 cells) (left). Maximum inhibition by the highest agonist dose (Log μM) (right). *$P < 0.05$ NFEPP at pH 6.5 vs 7.4; 2-tailed t test. Data are means ± SEM.

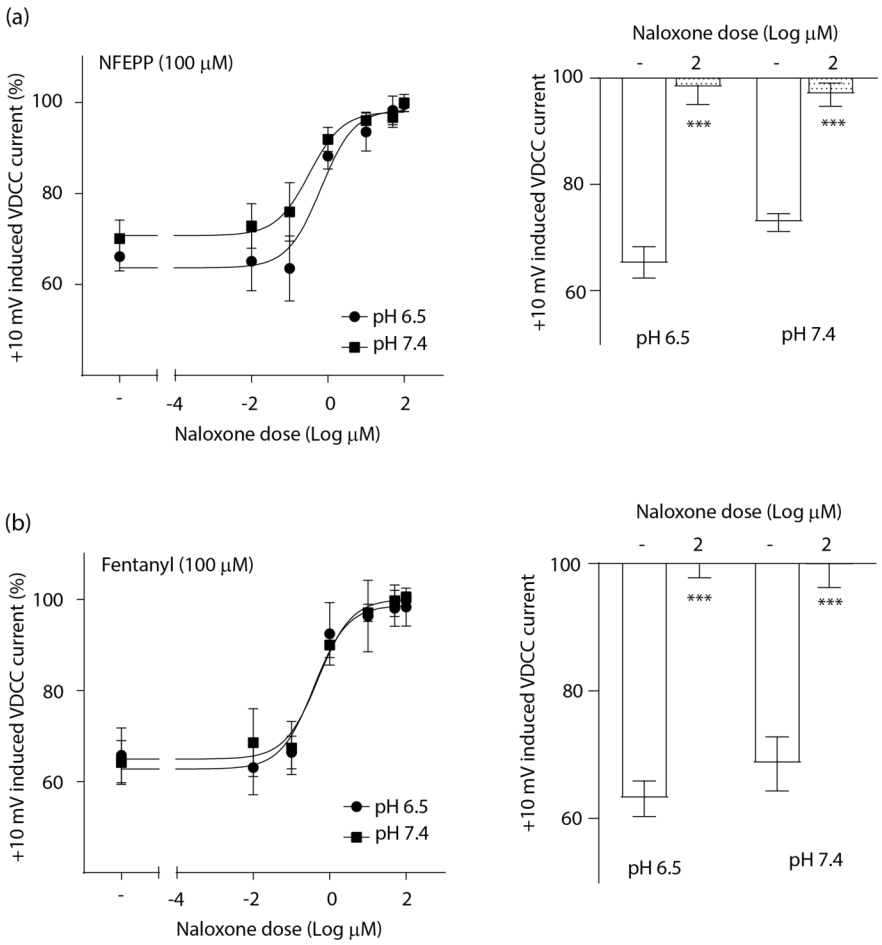

Figure 3

Dose-dependent effects of naloxone on the maximum inhibition of +10mV-induced calcium currents by NFEPP (a) or fentanyl (b) at pH 6.5 and pH 7.4 measured by patch clamp in isolated rat sensory neurons (N=16-20 cells) (left). Effects of the highest naloxone doses (Log μM) (right). ***P < 0.001 naloxone vs. control at pH 6.5 vs 7.4; 2-tailed t test. Data are means ± SEM.

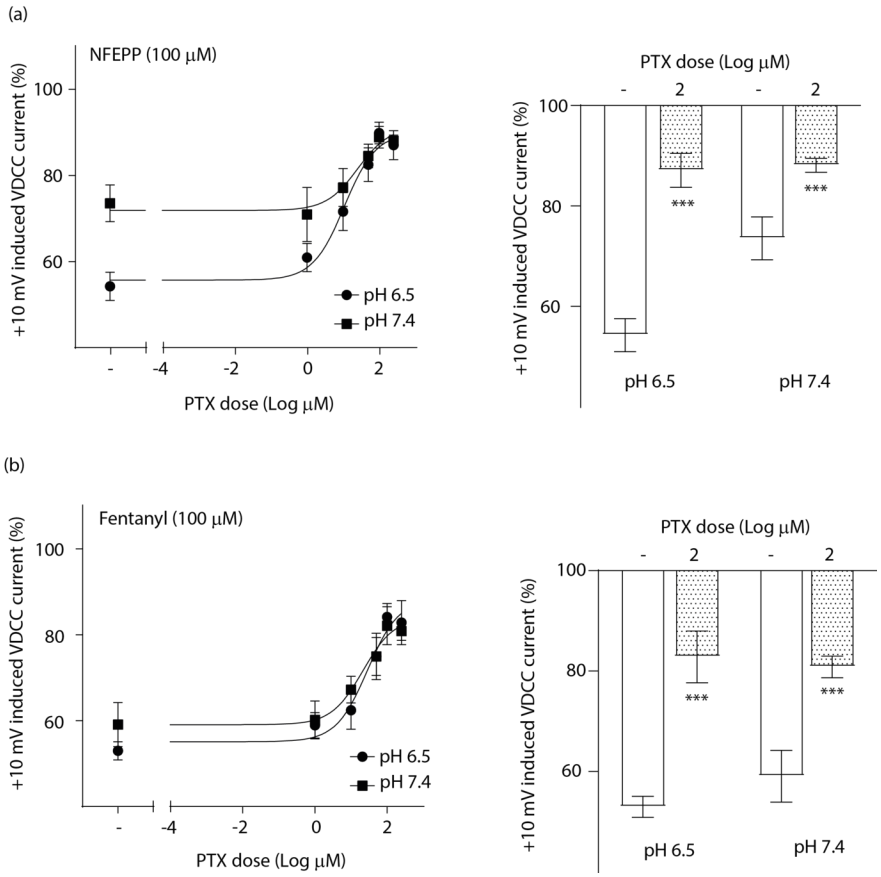

Figure 4

Dose-dependent effects of pertussis toxin (PTX) on the maximum inhibition of +10mV-induced calcium currents by NFEPP (a) or fentanyl (b) at pH 6.5 and pH 7.4 measured by patch clamp in isolated rat sensory neurons (N=17-22 cells) (left). Effects of the highest PTX doses (Log μM) (right). ***P $<$ 0.001 PTX vs. control at pH 6.5 vs. 7.4; 2-tailed t test. Data are means ± SEM.

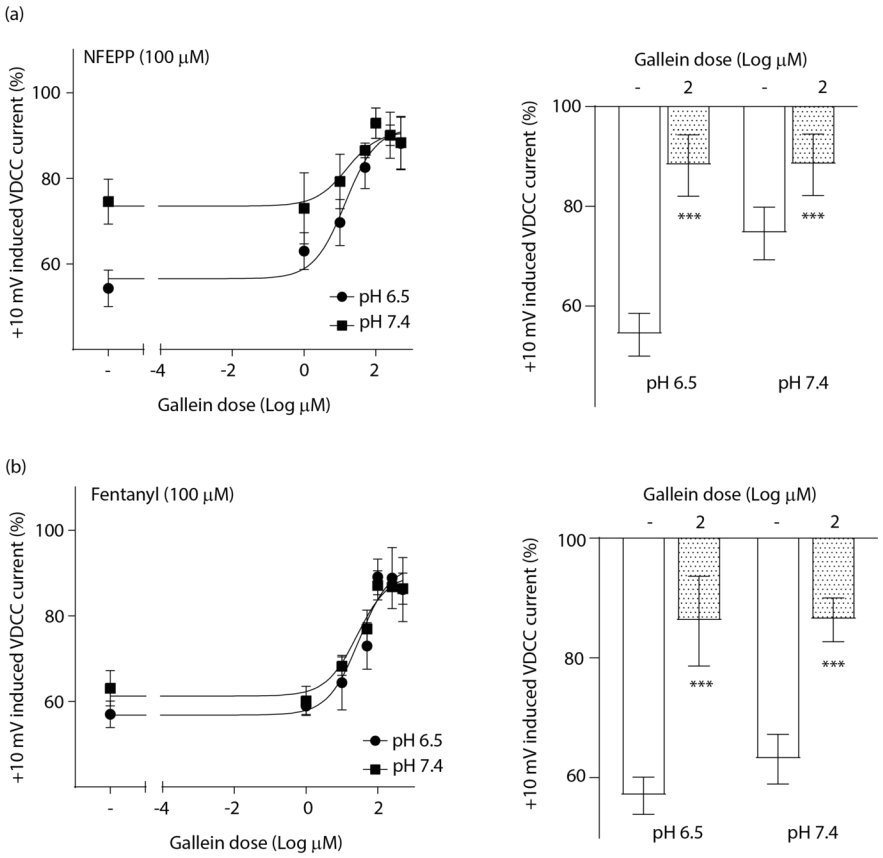

Figure 5

Dose-dependent effects of gallein on the maximum inhibition of +10mV-induced calcium currents by NFEPP (a) or fentanyl (b) at pH 6.5 and pH 7.4 measured by patch clamp in isolated rat sensory neurons (N=15-25 cells) (left). Effects of the highest gallein doses (Log μM) (right). ***P < 0.001 gallein vs control at pH 6.5 vs 7.4; 2-tailed t test. Data are means ± SEM.

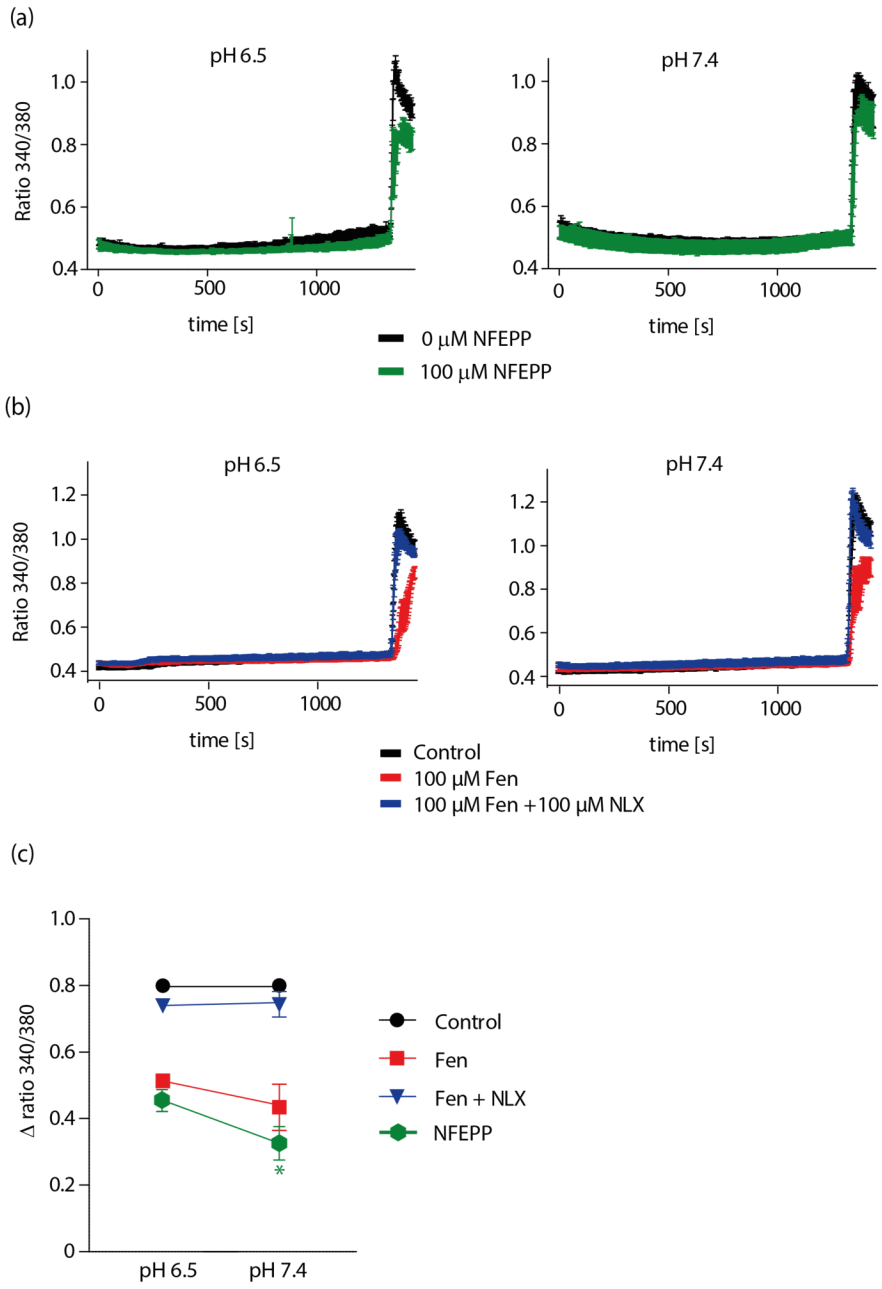

Figure 6

Inhibition of calcium signals by NFEPP at pH 6.5 in rat sensory neurons. (a) Fura-2 imaging experiments with rat sensory neurons treated with 100 µM NFEPP (green trace, N=259 neurons, 9 recordings from 3 rats) and non-treated (0 µM NFEPP) (black trace, N=256 neurons, 9 recordings from 3 rats) at pH 6.5 and pH 7. (b) Calcium responses in rat sensory neurons treated with 100 µM fentanyl (red trace, N=445 neurons, 18 recordings from 6 rats), treated with 100 µM fentanyl + 100 µM naloxone (blue trace, N=454 neurons, 18 recordings from 6 rats) and non-treated (vehicle control: DMSO) (black trace, N=463 neurons, 18 recordings from 6 rats) at pH 6.5 and pH 7. (c) Summary, delta ratio 340/360 from (a) & (b) at pH 6.5 and pH 7. *P $<$ 0.05 NFEPP at pH 6.5 vs 7.4; 2-tailed t test. Traces represent means ± SEM.

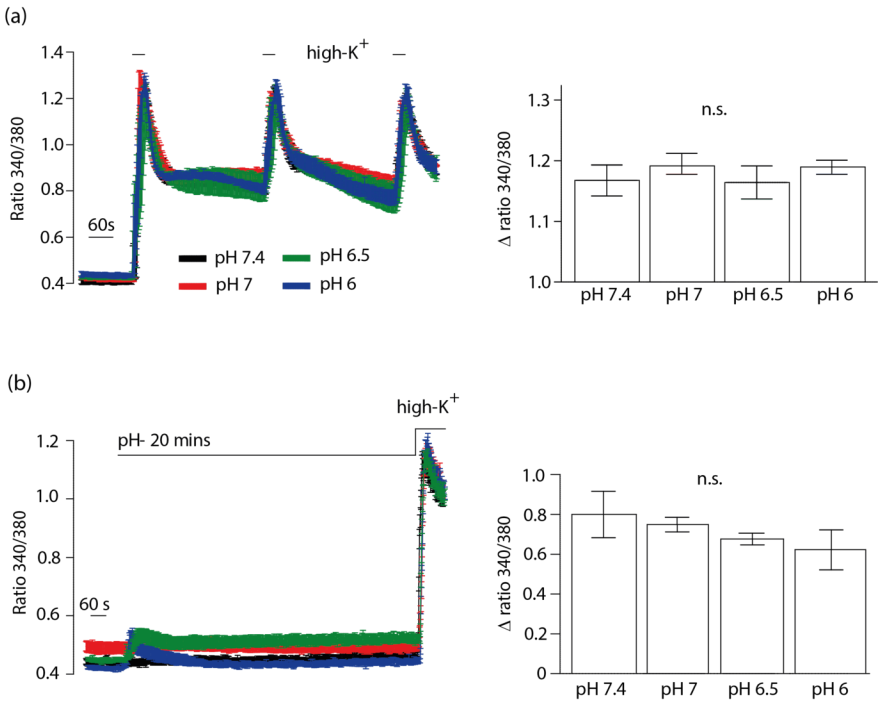

Figure 7

Effects of inflammatory pH conditions on calcium signals in rat sensory neurons. Fura-2 imaging experiments with rat sensory neurons treated with (a) short (60s) and (b) long (20 min) application of extracellular pH 7.4 (black trace, N=356 neurons), pH 7 (red trace, N=302 neurons), pH 6.5 (green trace, N=383 neurons) and pH 6 (blue trace, N=386 neurons). Twelve recordings for each pH from 4 rats (1 rat per pH) are shown. The right bar graphs represent delta ratio 340/380 for different pH values. $P > 0.05$; One-way ANOVA on ranks. Traces represent means ± SEM.

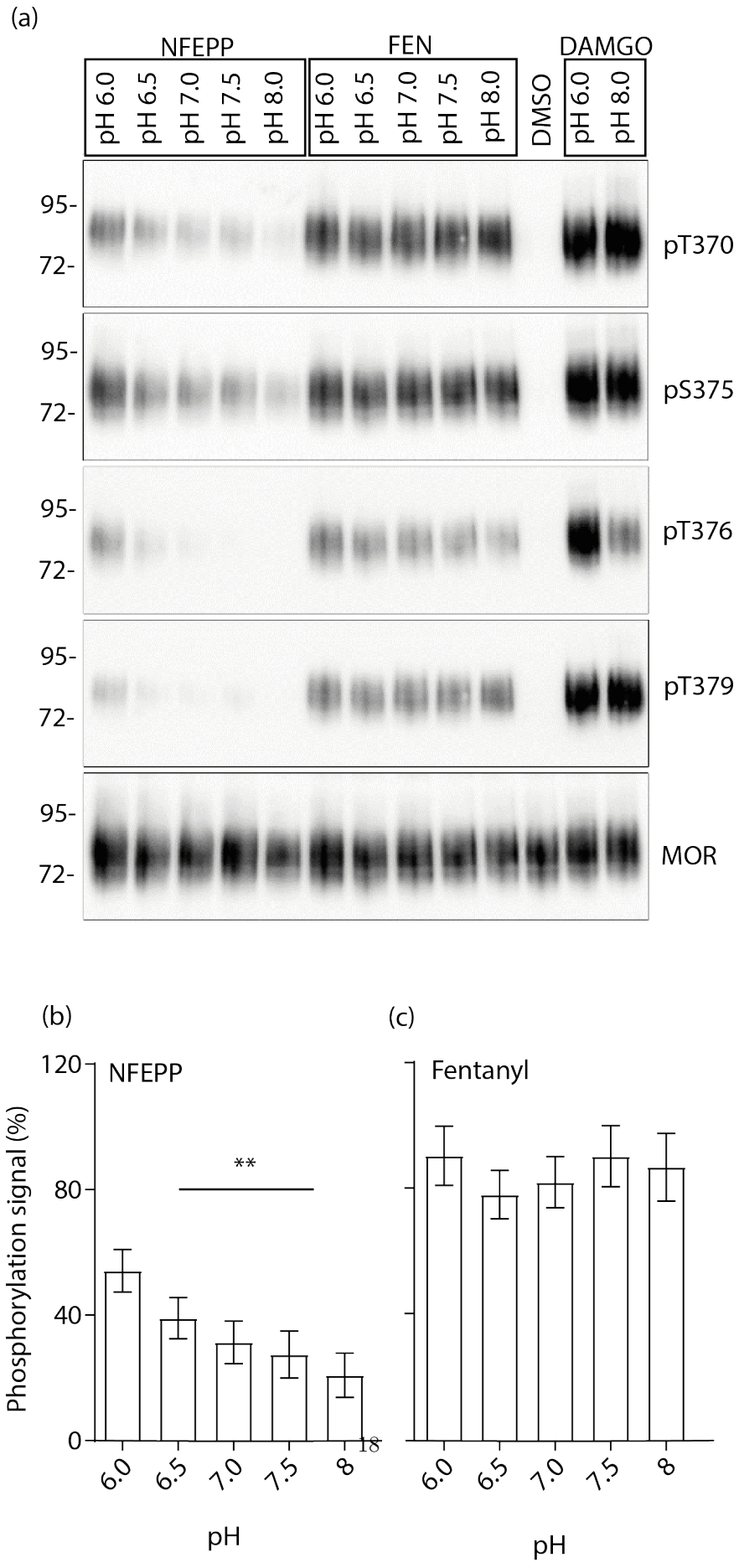

Figure 8

Effects of different pH values on NFEPP- or fentanyl-induced MOR phosphorylation in HEK293 cells. (a) MOR phosphorylation was analyzed with antibodies specifically reacting with phosphorylated residues T370, S375, T376 and T379. Controls were treated with 1 µM DMSO (negative control) or 10 µM DAMGO (positive control). Total phosphorylation signal recorded from residues (T370, S375, T376, T379) when stimulated with 1 µM NFEPP (b) or fentanyl (c) in a pH-dependent manner (N=16). **P < 0.01; One-way ANOVA on ranks (specific sample pairs are not analyzed). Data are means ± SEM.

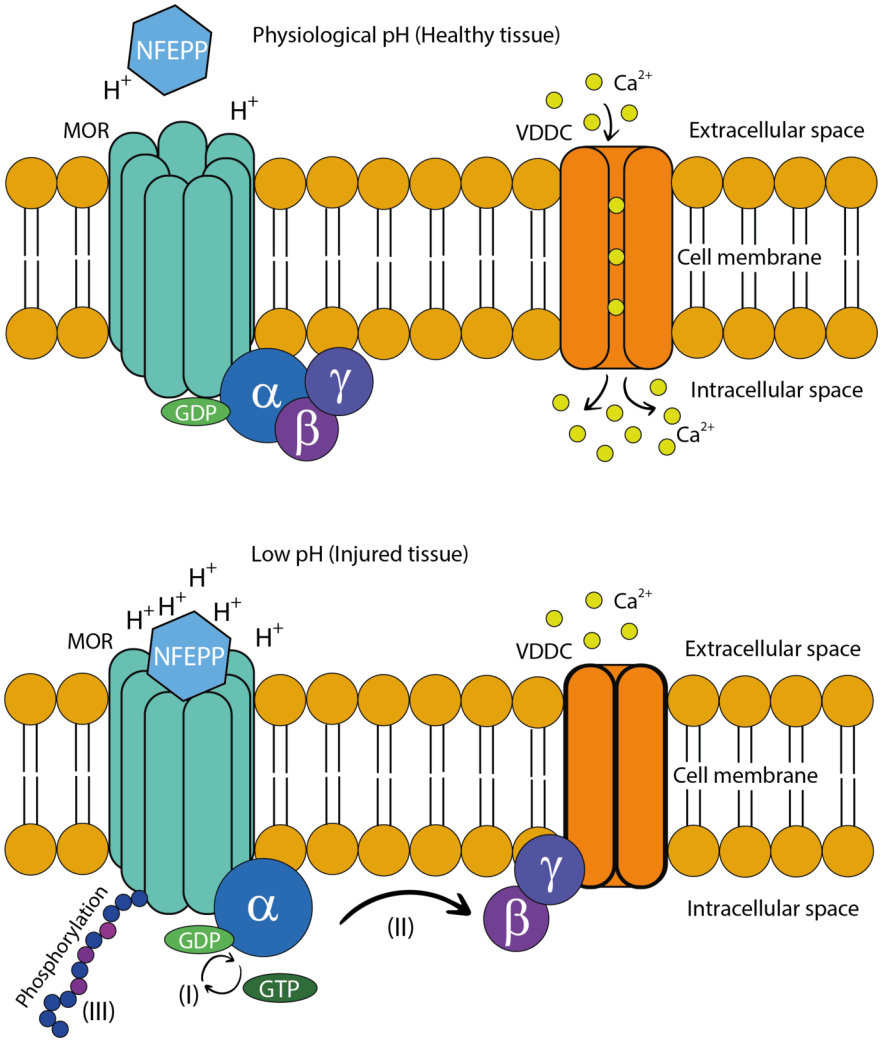

Graphical Abstract

Abbreviations

CNS: central nervous system

DAMGO: [D-Ala2,N-Me-Phe4,Gly5-ol]-enkephalin

GPCR: G-protein coupled receptor

HEK MOR-WT: HEK293 cells stably transfected with mu opioid receptor wild type

MOR: mu opioid receptor

NFEPP: (±)-N-(3-fluoro-1-phenethylpiperidine-4-yl)-N-phenyl propionamide

NLX: naloxone

pK_a: acid dissociation constant

PNS: peripheral nervous system

PTX: pertussis toxin

VDCC: voltage dependent calcium channel

M. Özgür Celik ORCID ID: 0000-0002-7706-4964

Viola Seitz ORCID ID: 0000-0002-8086-8090

Fatih Yergöz ORCID ID: 0000-0002-9709-8563

Sandeep Dembla ORCID ID: 0000-0003-2708-4390

Stefan Schulz ORCID ID: 0000-0002-5997-8885

Christoph Stein ORCID ID: 0000-0001-5240-6836